

Degradation of the cellulosic key chromophore 5,8-dihydroxy-[1,4]-naphthoquinone by hydrogen peroxide under alkaline conditions.

Nele Sophie Zwirchmayr, Takashi Hosoya, Ute Henniges, Lars Gille, Markus Bacher, Paul G. G. Furtmüller, and Thomas Rosenau

J. Org. Chem., **Just Accepted Manuscript** • DOI: 10.1021/acs.joc.7b01827 • Publication Date (Web): 02 Oct 2017

Downloaded from <http://pubs.acs.org> on October 4, 2017

Just Accepted

“Just Accepted” manuscripts have been peer-reviewed and accepted for publication. They are posted online prior to technical editing, formatting for publication and author proofing. The American Chemical Society provides “Just Accepted” as a free service to the research community to expedite the dissemination of scientific material as soon as possible after acceptance. “Just Accepted” manuscripts appear in full in PDF format accompanied by an HTML abstract. “Just Accepted” manuscripts have been fully peer reviewed, but should not be considered the official version of record. They are accessible to all readers and citable by the Digital Object Identifier (DOI®). “Just Accepted” is an optional service offered to authors. Therefore, the “Just Accepted” Web site may not include all articles that will be published in the journal. After a manuscript is technically edited and formatted, it will be removed from the “Just Accepted” Web site and published as an ASAP article. Note that technical editing may introduce minor changes to the manuscript text and/or graphics which could affect content, and all legal disclaimers and ethical guidelines that apply to the journal pertain. ACS cannot be held responsible for errors or consequences arising from the use of information contained in these “Just Accepted” manuscripts.

Degradation of the cellulosic key chromophore 5,8-dihydroxy-[1,4]-naphthoquinone by hydrogen peroxide under alkaline conditions

Nele Sophie Zwirchmayr[†], Takashi Hosoya[†], Ute Henniges[†], Lars Gille[‡], Markus Bacher[†], Paul Furtmüller[†], Thomas Rosenau^{†*}

*Corresponding author: thomas.rosenau@boku.ac.at

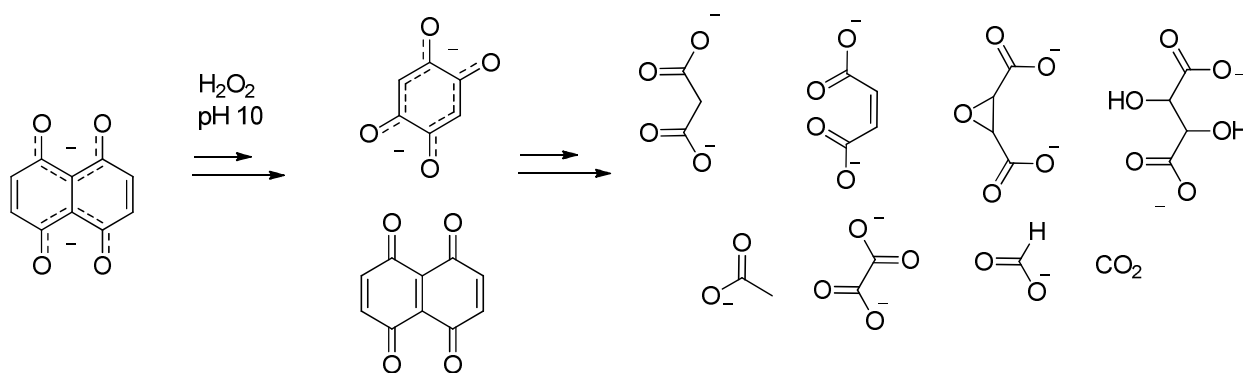
[†]Department of Chemistry, University of Natural Resources and Applied Life Sciences, Muthgasse 18, A-1190 Vienna, Austria

[‡]Department of Biomedical Sciences, University of Veterinary Medicine Vienna, Veterinärplatz 1, A-1210 Vienna, Austria

Keywords

Cellulose, chromophores, naphthoquinone, benzoquinone, 1,4,5,8-naphthalenetetrone, P-stage, pulp bleaching

Abstract graphic



Abstract

5,8-Dihydroxy-[1,4]-naphthoquinone (DHNQ) is one of the key chromophores in cellulosic materials. Its almost ubiquitous presence in cellulose makes it a target molecule of the pulp and paper industry's bleaching efforts. In the presented study, DHNQ was treated with hydrogen peroxide under alkaline conditions at pH 10, resembling the conditions of industrial hydrogen peroxide bleaching (P stage). The reaction mechanism, reaction intermediates and final degradation products were analysed by UV/Vis, NMR, GC-MS, and EPR. The degradation reaction yielded C₁- to C₄-carboxylic acids as the final products. Highly relevant for pulp bleaching are the findings on intermediates of the reaction, as two of them, 2,5-dihydroxy-[1,4]-benzoquinone (DHBQ) and 1,4,5,8-naphthalenetetrone, are potent chromophores themselves. While DHBQ is one of the three cellulosic key chromophores and its degradation by H₂O₂ is well established, the second intermediate, 1,4,5,8-naphthalenetetrone, is reported for the first time in the context of cellulose discolouration.

Introduction

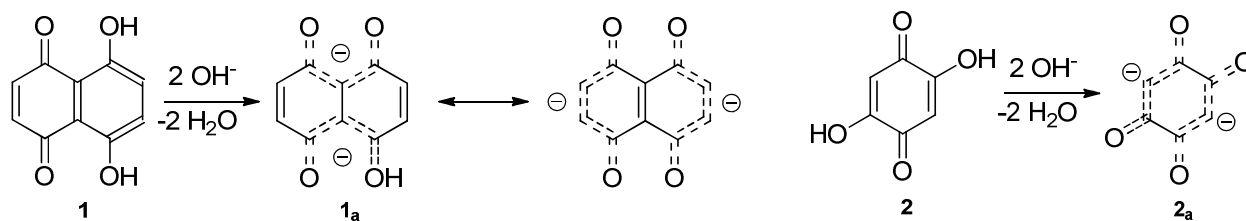
Chromophores in pulp and paper are caused by oxidative damage of the polysaccharide matrix during processing – especially oxidative bleaching – and subsequent aging processes. Residual lignin or extractives might also be involved as precursor compounds. Often these aging processes are summarized as “yellowing” or “brightness reversion”. In fully bleached pulps, the chromophore content can be as low as 0.1 ppm,¹ and already concentrations slightly higher result in a yellowish tint that is well discernible for the human eye. The pulp and paper industry is aiming for ultimately bright products and has a strong interest in reducing the chromophore content; at the same time bleaching sequences are optimised in order to reduce the amount of costly bleaching chemicals and to minimize oxidative damage to the cellulose. Similarly, conservators are interested in preserving their often valuable historic cellulosic documents endangered by darkening caused by high chromophore content. To meet all of these needs, the chromophores first had to be identified, as done so by application of the CRI (chromophore release and identification) method.^{2,3} This approach, for the first time, provided access to the chromophoric compounds in cellulose whereas before only likely structural units, such as conjugated carbonyl structures or quinones had been surmised. Comparison of the structures

1
2
3 allowed distinguishing between “primary” chromophores, originating from carbohydrate matter
4 or respective degradation products, and “secondary” chromophores, that involve process
5 chemicals in their formation, such as for instance sulfur species in rayon production. Within the
6 primary chromophores, the most predominant structures belong to the compound classes of
7 hydroxy-[1,4]-benzoquinones, hydroxy-[1,4]-naphthoquinones, and 2-hydroxy-acetophenones.
8 Of these groups, the three compounds 5,8-dihydroxy-[1,4]-naphthoquinone (DHNQ, **1**), 2,5-
9 dihydroxy-[1,4]-benzoquinone (DHBQ, **2**), and 2,5-dihydroxy-acetophenone have been found in
10 all materials analysed and have become known as the three cellulosic key chromophores.¹
11

12
13
14
15
16
17
18
19
20
21
22
23
24
25
26
27
28
29
30
31
32
33
34
35
36
37
38
39
40
41
42
43
44
45
46
47
48
49
50
51
52
53
54
55
56
57
58
59
60

Once main culprits in cellulose discolouration had been determined, establishing the
chromophores’ reactivities towards common bleaching agents used in the pulp and paper
industry would be a prerequisite to optimizing bleaching sequences and developing methods for
preservation of historic paper documents. DHBQ has been subjected to in-depth analyses
regarding its reaction mechanism and products when degraded by H₂O₂ under non-buffered and
alkaline conditions. It was found that the main degradation products are carboxylic acids, namely
malonic acid and acetic acid, as well as carbon dioxide,^{4,5} resulting from a multi-step sequence
with peroxide addition and β-scission as the main reactions. Similarly to DHBQ, the chemistry
of DHNQ has been investigated regarding its potential in organic synthesis and has been
reviewed recently.⁶ However, it has not yet been examined concerning its degradation and
reactivity towards bleaching agents, such as hydrogen peroxide, ozone, and chlorine dioxide.

Both, DHNQ and DHBQ are readily deprotonated in alkaline media, and their anions (**1_a** and **2_a**
in Scheme 1) exhibit strong resonance stabilisation and thus delocalised double bonds. This
resonance stabilisation is the key issue when investigating the fate of DHNQ in bleaching
sequences: common bleaching agents attack localised double bonds and disrupt the quinoid
electronic structure of the chromophore, finally leading to colourless products. In the case of
delocalized double bonds - as in **1_a** and **2_a** - degradation becomes much slower and bleaching
efforts less effective.



Scheme 1. DHNQ (**1**) and DHBQ (**2**) form highly resonance-stabilized anions, **1_a** and **2_a**, respectively, in alkaline media.

Another reason for the peculiar stability of DHNQ is its high thermodynamic stabilisation that results in its easy reformation from C2 to C4 fragments, namely degradation products of cellulosic materials formed in bleaching sequences.⁶ Summing up, DHNQ is not only resistant to bleaching efforts, but it is also reformed easily, making its successful and lasting removal from pulp and other cellulosic matter particularly difficult.

In the present study, the key chromophore DHNQ, was degraded by H₂O₂ under alkaline conditions at pH 10 that resemble a P stage in industrial bleaching.⁵ An emphasis was put on the intermediates and degradation products formed. Kinetic analyses of the DHNQ/H₂O₂ reaction were performed and the (radical) intermediates analysed with the help of *in situ* NMR and EPR experiments. The reaction mechanism of DHNQ/H₂O₂ is presented in detail. Final support of the shown intermediates and reaction mechanism is achieved in form of quantum chemical calculations, by calculation of activation parameters and comparison with experimental values.

Results and discussion

Kinetic analysis and quantum chemical calculations.

In previous studies on the chromophore DHBQ and its degradation by H₂O₂ at different pH values (unbuffered and mildly alkaline at pH 10),^{4,5} it was shown that the reaction followed a pseudo-first order. The requirements to define reactions as pseudo-first order are (1) one of the reagents is present in such a large excess that its concentration can be considered constant in the course of the reaction and (2) a linear correlation for ln(A) vs. time is found. Applied to our case, the integrated rate law for pseudo-first order reactions is as given in eq. 1, with [DHNQ]₀ being the initial concentration of DHNQ and *k* being the kinetic rate constant.^{4,7}

$$[\text{DHNQ}] = [\text{DHNQ}]_0 e^{-kt} \quad \text{[equation 1]}$$

The DHNQ/H₂O₂ degradation was followed in stopped-flow UV/Vis measurements with excesses of H₂O₂ between 5 and 667 molar equivalents in relation to DHNQ. Based on previously recorded UV/Vis spectra of DHNQ at pH 10, the peak at 574 nm was chosen for the kinetic analysis. A linear correlation was found for ln(A) against time for all excesses of H₂O₂, meaning that a pseudo-first order was found in all DHNQ degradation reactions.

The reaction constant *k* can be obtained from the slope of the plot ln(A) against time. This was done so for the first 100 s (equivalents of H₂O₂ from 5 to 333) or the first 50 s (equivalents of 500 and 667). Plotting longer reaction times distorted the clearly linear, ideal correlation obtained for 50 s to 100 s; a phenomenon that is commonly known to occur due to follow-up reactions (or “competing” reactions).⁷ For results on *k* at 298.15 K and the graph ln(A) vs. time, see Figure 1.

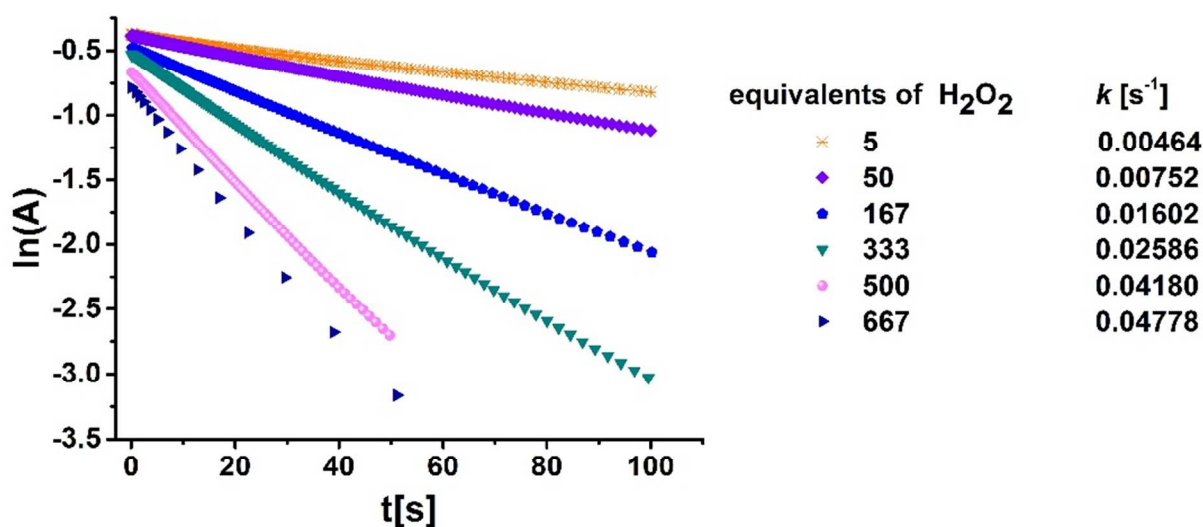


Figure 1. Degradation of DHNQ by H₂O₂ at 298.15 K followed by UV/Vis analysis at 576 nm, measured in stopped-flow mode. The obtained linear correlation for ln(A) vs. time *t* indicates a pseudo-first reaction order for all molar equivalents of H₂O₂ used. The reaction rate constant *k* was obtained from the slope of the corresponding lines.

In addition to stopped-flow UV/Vis measurements, temperature-regulated UV/Vis measurements were done to determine the activation energy ($E_{A(\text{exp})}$) of the rate-determining step of the DHNQ/ H_2O_2 degradation. With the knowledge on the reaction rate obtained from the stopped-flow UV/Vis measurements – a fast reaction, only exhibiting ideal behaviour for the first 50 to 100 seconds of the reaction – a 100-fold molar excess of H_2O_2 (relative to DHNQ) was chosen for the manually operated, temperature-regulated UV/Vis experiments. This way, the reaction was already reasonably fast at lower temperatures, and measurements were still possible at higher temperatures. The absorption was again followed at 576 nm, and the reaction temperatures ranged between 303.15 and 343.15 K. $\ln(A)$ was plotted against time for reaction times of up to 200 s, depending on temperature and the resulting linear range. The k values obtained from the slopes of the lines ranged between 0.00396 and 0.0351 s^{-1} . An Arrhenius plot was constructed from $\ln(k)$ vs. $1/T$, as depicted in Figure 2. The experimental activation energy $E_{A(\text{Exp})}$ was calculated from the slope of the Arrhenius plot and determined to be 11.7 kcal/mol.

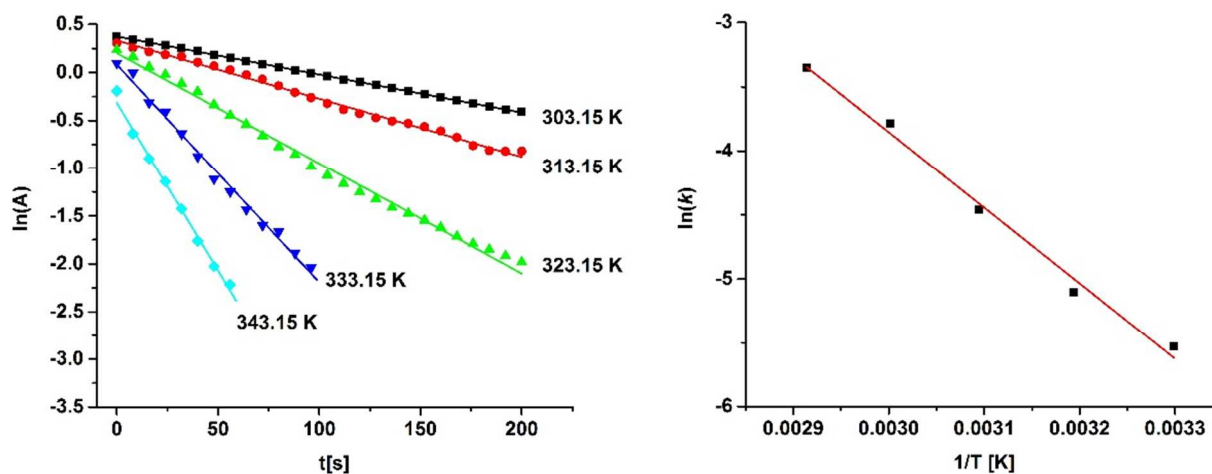


Figure 2. Left: $\ln(A)$ vs. time t at 303.15 to 343.15 K, determined by UV/Vis analyses at 576 nm. k was determined from the slope of the lines and used for construction of the Arrhenius plot. Right: Arrhenius plot obtained from $\ln(k)$ vs. $1/T$ [K]. The slope, being equal to $-E_A/R$, was used in the calculation of $E_{A(\text{Exp})}$.

The activation parameters ($\Delta^\ddagger H^\circ$, $\Delta^\ddagger S^\circ$, and $\Delta^\ddagger G^\circ$) were calculated based on $E_{A(\text{Exp})}$ ⁸ and are presented in Table 1. Additionally, an Eyring plot was constructed by plotting $\ln(k/T)$ vs. $1/T$. From the intercept, $\Delta^\ddagger S^\circ$ was calculated. The Eyring value for $\Delta^\ddagger S^\circ$ (-33.12 cal/K·mol) was in

good accordance with the values of $\Delta^\ddagger S^\circ$ calculated from $E_{A(\text{Exp})}$, which ranged between -32.83 and -33.26 cal/K·mol. Variation of the values of $\Delta^\ddagger H^\circ$, $\Delta^\ddagger S^\circ$, and $\Delta^\ddagger G^\circ$ with temperature is minimal. Noteworthy, $\Delta^\ddagger G^\circ$ is about twice as large as $\Delta^\ddagger H^\circ$. With the well-known Gibbs-Helmholtz equation $\Delta^\ddagger G^\circ = \Delta^\ddagger H^\circ + T\Delta^\ddagger S^\circ$ in mind, this indicates a large entropic influence and that the degree of order in the rate-determining transition state is higher than that of the reactants. This makes it highly likely that the rate-determining step is intermolecular, involving both DHNQ and a coreactant – evidently H_2O_2 or a derived species – rather than a subsequent fragmentation. The latter, as an intramolecular process, would have a (small) positive activation entropy.

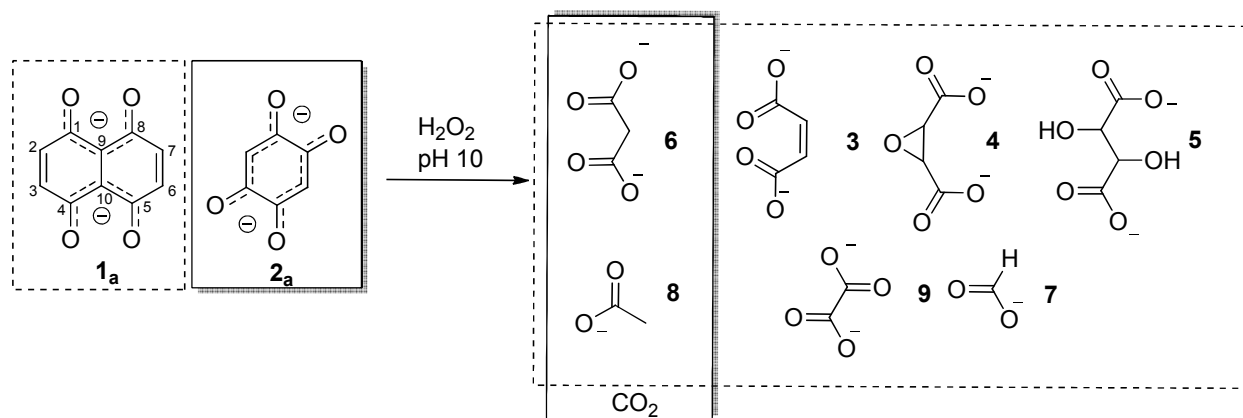
Table 1. Experimental pseudo-first order rate constants k at different reaction temperatures (313.15 to 343.15 K), obtained by UV/Vis measurements, and the activation parameters $\Delta^\ddagger H^\circ$, $\Delta^\ddagger S^\circ$, and $\Delta^\ddagger G^\circ$ as obtained from the Eyring plot, $\ln(k/T)$ vs. $1/T$. For comparison, the Arrhenius activation energy $E_{A(\text{Exp})}$, calculated from the slope of the Arrhenius plot, was 11.7 kcal/mol. $\Delta^\ddagger S^\circ$ calculated from the intercept of the x-axis of the Eyring plot was -33.12 cal/K·mol.

Temperature [K]	k [s^{-1}]	activation parameters		
		$\Delta^\ddagger H^\circ$ [kcal/mol]	$\Delta^\ddagger S^\circ$ [cal/K·mol]	$\Delta^\ddagger G^\circ$ [kcal/mol]
303.15	0.00396	11.14	-32.83	21.09
313.15	0.00607	11.12	-33.28	21.54
323.15	0.01152	11.10	-33.23	21.83
333.15	0.02275	11.08	-33.03	22.08
343.15	0.0351	11.06	-33.26	22.47

Degradation product analysis.

For degradation product analysis, a bulk degradation experiment was conducted under similar conditions as the UV/Vis analyses. **1** was dissolved in borax buffer (pH 10) and H_2O_2 was added (195 equivalents). Upon complete decolouration of the initially dark blue reaction solution, the solution was freeze-dried and the remaining solid was subject to different analyses, ^1H , 2D NMR (HSQC/HMBC), and GC-MS. Additionally, *in situ* NMR experiments were performed at a smaller scale, using D_2O and 30 equivalents of H_2O_2 . The products detected by NMR were

maleic acid (**3**), oxirane-2,3-dicarboxylic acid (**4**), malonic acid (**6**), formic acid (**7**), and acetic acid (**8**) (the latter only in traces after lyophilisation), and were confirmed by comparison with authentic samples. Compound **7** was only found in the *in situ* experiment, as its high volatility renders it impossible to detect it after the sample work-up that involves lyophilisation. GC-MS analyses confirmed the products **3** and **6**. GC-MS revealed another degradation product, oxalic acid (**9**). Compound **9** is formed from oxidation of the intermediate tartaric acid (**5**) - the hydrolysate of **4**. Because product **9** lacks any non-exchangeable protons, it cannot be detected in ^1H NMR. The degradation products of DHNQ/ H_2O_2 under alkaline conditions are depicted in Scheme 2.

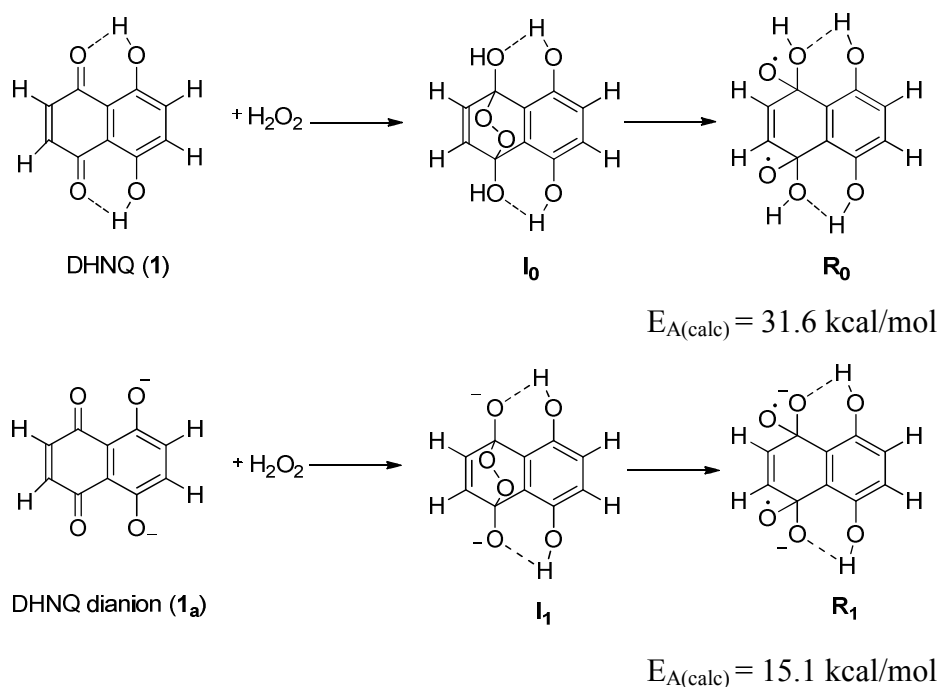


Scheme 2. Alkaline degradation of **1** or **2** by H_2O_2 , resulting in similar degradation products. Product **3** is formed by β -scission of the "quinoid" side of **1_a** and compounds **4**, **7**, and **9** result from **3** in the presence of H_2O_2 . Compounds are depicted as their (di)anions.

Degradation mechanism and quantum chemical calculations.

Based on degradation product analysis and UV/Vis, a reasonable degradation mechanism can be conceived as follows: the formation of **3** originates from the loss of DHNQ's "quinoid part" – a strong indicator being that only **3** as the *cis*-isomer of the two butenedioic acids was found, but not the *trans*-configured counterpart, fumaric acid. **4** can be easily formed from **3** in the presence of an oxidizer.^{9,10} The similarity of the other degradation products obtained from DHNQ and the degradation products of DHBQ is evident^{4,5} - DHNQ equally results in **6** and **8** when degraded with H_2O_2 . Is it thus highly likely that DHBQ is an intermediate in the degradation of DHNQ, even more when taking into account that **4**, **7**, and **9**, are all linked by originating from **3**.

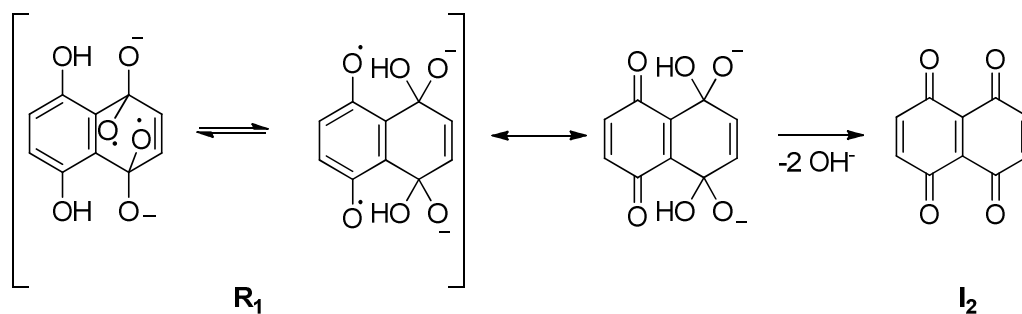
As concluded from the kinetic analysis, the reaction of DHNQ and H₂O₂ follows pseudo-first order kinetics, and the rate-determining first step is the attack of DHNQ by H₂O₂. The reactions's first intermediate is formed by addition of H₂O₂ to the "quinoid" half of the molecule. In other words, the attack of H₂O₂ cancels the resonance stabilization – the superposition of quinoid and aromatic canonic forms – and forces the molecule to "decide" which half is aromatic and which quinoid, the latter reacting with the oxidant.⁵ Depending on the medium, and thus the resulting charge of DHNQ, this results in the formation of **I**₀ (from neutral DHNQ) or **I**₁ (from the dianion), and the subsequent scission of the instable peroxide linkage between C1 and C4 results in either a bi-radical **R**₀ or a bis(anion radical) **R**₁, see Scheme 3. Quantum chemical calculations for the formation of **R**₀ and of **R**₁ were carried out on the DFT(M062x) level. The values for the calculated activation energy E_{A(calc)} were compared with the experimental one, E_{A(exp)}. E_{A(calc)} for **R**₁ matches the experimental one very well, with values of 15.1 kcal/mol and 11.7 kcal/mol, respectively. E_{A(calc)} for **R**₀ (neutral), however, is almost twice as high as the experimental one, 31.6 kcal/mol. Thus, deprotonation of **1**, leading to **1**_a, takes place before H₂O₂ addition, and scission of the rather labile endoperoxide between C1 and C4 in intermediate **I**₁ results in biradical **R**₁.



Scheme 3. Intermediates **I**₀, **I**₁, **R**₀, and **R**₁ depicted as used in the quantum chemical calculations. For the formation of **R**₁, the calculated E_A (15.1 kcal/mol) matches the experimental

value (11.7 kcal/mol) quite well. Compared to the anion, attack of H_2O_2 to neutral DHNQ is much disfavoured. DHNQ is thus present in its deprotonated form before H_2O_2 addition, and scission of the endoperoxide linkage in the resulting intermediate \mathbf{I}_1 leads to the highly transient bis(anion radical) \mathbf{R}_1 .

The good match of the calculated and experimental E_A values is a strong back-up for the proposed structure of the short-lived intermediate \mathbf{R}_1 . By tautomerisms ([1,5]-sigmatropic proton shifts) and single-electron transfer – both occurring twice due to the biradical character – a dianionic intermediate is formed that immediately loses two hydroxide anions to form 1,4,5,8-naphthalenetetrone (\mathbf{I}_2) as a stable intermediate (Scheme 4). All conversions between \mathbf{R}_1 and \mathbf{I}_2 are exergonic (spontaneous) and do not exhibit any significant activation energy barriers compared to the rate-determining step discussed above. 1,4,5,8-Naphthalenetetrone is a strong chromophore itself. So far, its occurrence has not been linked to chromophores in cellulosics.

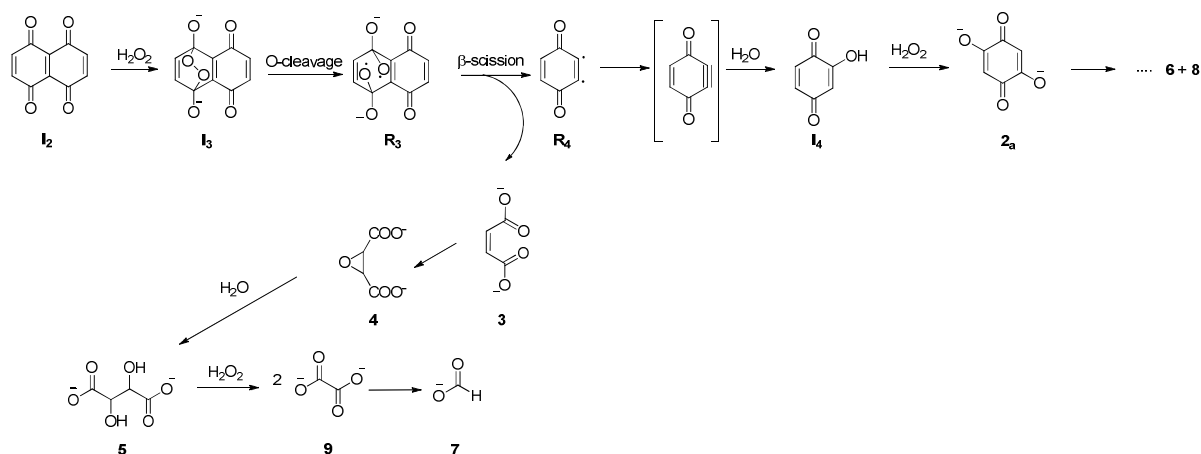


Scheme 4. Formation of the stable, chromophoric intermediate \mathbf{I}_2 from transient bis(anion radical) \mathbf{R}_1 .

Experimental confirmation that \mathbf{I}_2 is truly an intermediate in the degradation of DHNQ by H_2O_2 , was provided by synthesis of an authentic sample of \mathbf{I}_2 according to a literature procedure.¹¹ In an *in situ* NMR experiment \mathbf{I}_2 was then degraded by H_2O_2 under the same conditions as DHNQ (borax buffer pH 10, 10 molar equivalents of H_2O_2). The same degradation products and the same product pattern were found in both cases: products **3**, **4**, **6**, **7**, and **8**, while **9** was detected only by GC-MS; **9** as it lacks protons visible in ^1H NMR. This outcome is only possible if \mathbf{I}_2 was indeed an intermediate in the course of the degradation of DHNQ by H_2O_2 .

The further degradation of **I**₂, as shown in Scheme 5, involves addition of hydrogen peroxide to form endoperoxide **I**₃. Cleavage of the labile O-O bond – analogous to **I**₁-**R**₁ – results in **R**₃ which undergoes immediate β-scission of **R**₃ into compound **3**, a detectable product, and **R**₄. **R**₄ immediately forms a highly reactive aryne species that adds water to give 2-hydroxy-1,4-benzoquinone **I**₄, which is known to be readily oxidized to DHBQ (**2**_a) in the presence of H₂O₂. From **2**_a, the degradation continues according to well-studied and already established pathways.⁵ Interestingly, DHBQ, a cellulosic key chromophore itself, was found as relatively stable intermediate in the degradation of DHNQ. Since both chromophores are found accompanying each other in cellulosic materials, this poses the interesting question if at least a part of the total DHBQ might originate from oxidative degradation of DHNQ. That the whole amount of DHBQ can be traced back to DHNQ can safely be excluded because DHBQ is also formed by other, already established pathways – e.g. from glucuronoxylan-derived hexeneuronic acids¹² or from “3-keto-glucose moieties” in oxidatively damaged cellulose chains.^{13,14}

Product **3** is further oxidized to **4**. In experiments with authentic samples, **4** did show signs of hydrolysis, albeit being fairly stable. Its hydrolysate, tartaric acid (**5**), is the intermediate in the formation of **9** and **7**. The degradation pathway **5-9-7** was also reported in literature.¹⁵



Scheme 5. Mechanism of the further degradation of 1,4,5,8-naphthalenetetrone (**I**₂) by H₂O₂ at pH 10 to colorless low-molecular weight compounds.

EPR measurements.

To gain further information about the degradation of DHNQ by H_2O_2 , the reaction was analysed by EPR. For this, the reaction conditions had to be adjusted: a more concentrated solution of **1** was prepared by using a 1:1 mixture of borax buffer (pH 10) and acetonitrile (MeCN), the final concentration being 28 mM. To slow the reaction down, only 5 molar equivalents of H_2O_2 were used. Under the applied conditions two radicals of different stability were detected, one being stable for several minutes, the other showing a remarkably high stability of several days at room temperature (Figure 3). The less stable radical appeared as a triplet signal, the more stable radical resulted in a singlet. The triplet signal was detected first and, upon its decline, the singlet appeared. However, this does not automatically mean that the intermediates giving the signals are formed in a chronological order - the singlet signal could have been present from the beginning of the measurement, but concealed by the triplet signal.

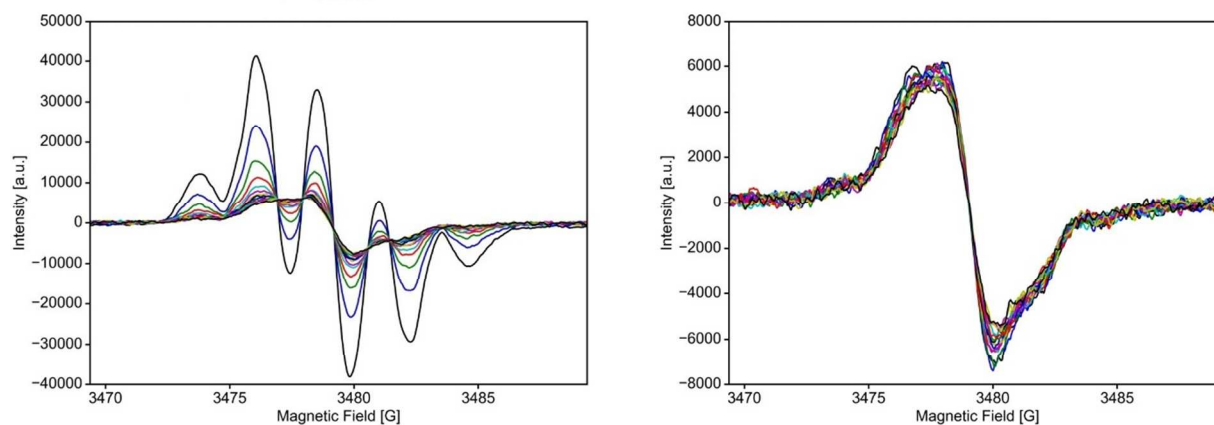


Figure 3. EPR signals of the radical intermediates detected upon the degradation of **1** by H_2O_2 . The triplet signal (left) declined within minutes, whereas the singlet signal of the more stable second intermediate (right) was still detectable after keeping the solution at room temperature for 6 days.

To be able to take these EPR results into account, it had to be confirmed that the altered conditions, namely changing solvent composition, had no influence on the degradation mechanism. The most feasible way was to perform *in situ* NMR experiments under EPR conditions (borax buffer pH 10: MeCN = 1:1; 5 equivalents H_2O_2) and to compare the obtained spectra to spectra obtained from the bulk degradation experiments (pH 10, 195 equivalents

1
2
3
4
5
6
7
8
9
10
11
12
13
14
15
16
17
18
19
20
21
22
23
24
25
26
27
28
29
30
31
32
33
34
35
36
37
38
39
40
41
42
43
44
45
46
47
48
49
50
51
52
53
54
55
56
57
58
59
60

H₂O₂). By making use of a water suppression technique, we were indeed able to confirm the formation of the products **3**, **4**, and **7**. The MeCN resonance was not suppressed, thus the peaks of the products **8** and **6** are superimposed by the strong solvent signal and were not visible. The degradation products **3**, **4**, and **7** were found in both reaction set-ups with comparable intensities, thus no influence of the MeCN addition on the degradation reaction's mechanism was observed. Additionally, two broad peaks were found at 7.27 and 6.25 ppm, most likely representing the radical giving the long-lived singlet in EPR. Comparison of the EPR signals with literature indicated that the structures giving the signals in EPR are both quinoid molecules.^{16,17} A first simulation¹⁸ revealed good accordance between an EPR spectrum for a quinoid species with (2+2) equivalent protons and the triplet obtained (Figure 4). **R**₁ forms **R**₂, a process where quick recombination of the two radicals with concomitant tautomerisms causes the EPR signal to disappear, as depicted in Scheme 3.

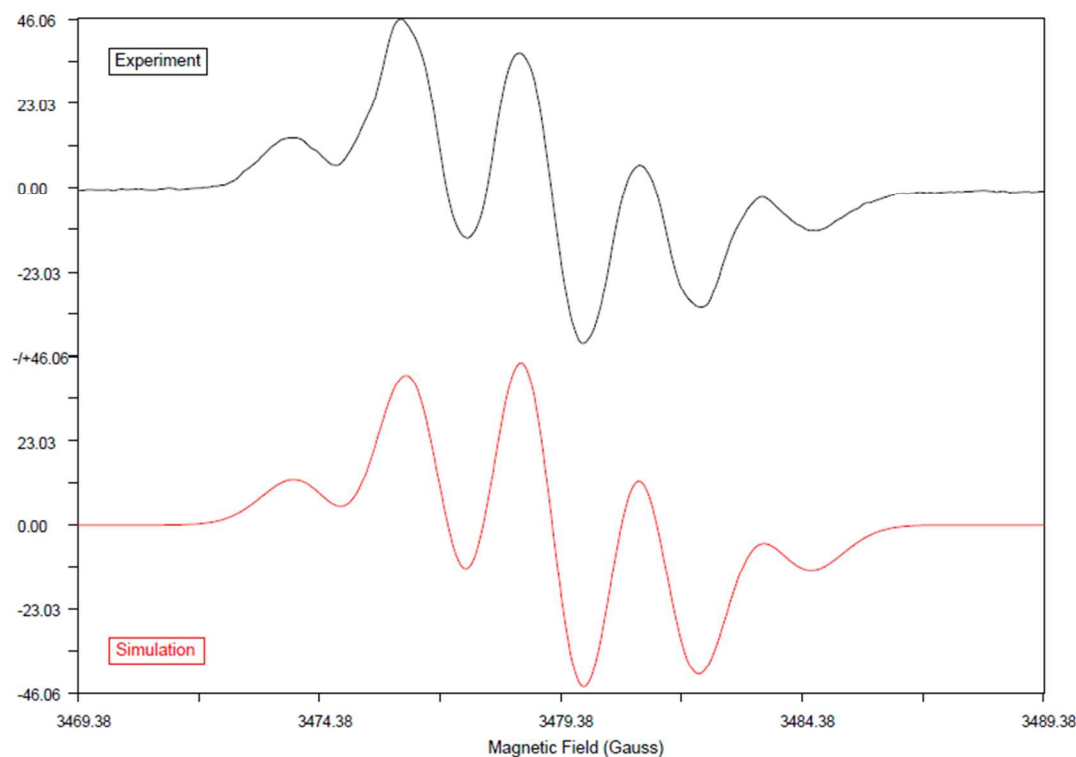


Figure 4. EPR signal of **R**₁, immediately after addition of H₂O₂ to the chromophore solution (top). The simulation for 4 (2+2) equivalent protons (bottom) is in good accordance with the experimental results.

1
2
3
4
5
6
7
8
9
10
11
12
13
14
15
16
17
18
19
20
21
22
23
24
25
26
27
28
29
30
31
32
33
34
35
36
37
38
39
40
41
42
43
44
45
46
47
48
49
50
51
52
53
54
55
56
57
58
59
60

At this point of the investigation we can ascertain that the stable radical species possesses 4 (2+2) equivalent protons, whether it is a species formed by one-electron oxidation of **1**, one-electron reduction of **I**₂ or whether it is **R**₃ cannot be conclusively decided in the moment. In all of these species the single spins are stabilized by resonance.

Conclusion

To summarize, the main products formed in the degradation of **1** by H₂O₂ at pH 10 are maleic acid (**3**), oxirane-2,3-dicarboxylic acid (**4**), and malonic acid (**6**), the latter originating from DHBQ which is formed as an intermediate in the DHNQ/H₂O₂ degradation. Minor products formed are oxalic acid (**9**), formic acid (**7**), tartaric acid (**5**) and acetic acid (**8**), which is originating from DHBQ as does **6**. Activation parameters were: E_A (from Arrhenius plot) = 11.7 kcal/mol. Δ[‡]S° (from Eyring plot) = 33.12 cal/K·mol. Δ[‡]H° = 11.14 to 11.06 kcal/mol, Δ[‡]S° = -32.38 to -33.26 cal/K·mol, and Δ[‡]G° = 21.09 to 22.47 kcal/mol. We were able to show that DHNQ can be fully degraded by H₂O₂ to colorless products. In the course of the degradation reaction, two other potent chromophores are formed: DHBQ, well-known to be a cellulosic key chromophore itself, and 1,4,5,8-naphthalenetetrone that was now reported in celluloses' chromophore chemistry for the first time. Applying the results of this study to industrial bleaching conditions, it must be pointed out that successful bleaching of any cellulosic material relies on sufficiently high excesses of H₂O₂ present in the bleaching sequence to ensure the degradation of not only DHNQ, but its follow-up chromophores, DHBQ and 1,4,5,8-naphthalenetetrone. This study covers only hydrogen peroxide as the bleaching agent. The behaviour of DHNQ towards other bleaching agents, such as ClO₂, ozone or peracetic acid, is the subject of current studies and upcoming reports.

Experimental section

General Experimental Methods. Commercial chemicals were of the highest grade available and were used without further purification. Reagent-grade solvents were used for all extractions and workup procedures. Distilled water was used for all aqueous solutions. The stopped-flow apparatus (model SX-18MV) was from Applied Photophysics (Surrey, UK). For the 20 μL

1
2
3 optical observation cell with 10 mm light path length, the dead time of the instrument is 1.2 ms.
4
5 Temperature-regulated UV/Vis spectra were recorded on a Hitachi U-3010 with a path length of
6
7 10 mm, slit width was 2 mm. GC-MS analysis was performed on an Agilent 7890A gas
8
9 chromatograph coupled with an Agilent 5975C triple axis mass selective detector (MSD; Agilent
10
11 Technologies, Santa Clara, CA, USA). A DB5-MS column (30 × 0.25 mm i.d. × 0.25 μm film
12
13 thickness; J&W Scientific, Folsom, CA, USA) was used. For ¹H NMR analysis, a Bruker
14
15 Avance II 400 instrument (¹H resonance at 400.13 MHz, ¹³C resonance at 100.61 MHz) with a 5
16
17 mm broadband probe head (BBFO) equipped with z-gradient with standard Bruker pulse
18
19 programs was used. Data were collected with 32k data points and apodized with a Gaussian
20
21 window function (GB = 0.3) prior to Fourier transformation. A 2.5 s acquisition time and a 1 s
22
23 relaxation delay were used. Bruker TopSpin 3.5 was used for the acquisition and processing of
24
25 the NMR data. EPR spectra of the DHNQ reaction intermediates were measured with a Bruker
26
27 EMX X-band spectrometer equipped with a TE cavity.

28
29 *Stopped-flow UV/Vis kinetic analysis.* All measurements were performed at 25°C and pH = 10 in
30
31 borax buffer, using a 0.6 mM solution of **1** with H₂O₂ concentrations between 30 to 400 mM
32
33 (corresponding to molar equivalents of H₂O₂ between 5 and 667). Measurement times were
34
35 ranging between 100 to 1000 s. The range recorded was 193-739 nm, step size was 2.2 nm.

36
37 *Temperature-regulated UV/Vis kinetic analysis.* A 0.2 mM solution of **1** was put in a covered
38
39 quartz cuvette and the temperature adjusted to the corresponding value (313.15 to 343.15 K).
40
41 After 10 minutes of equilibration time, H₂O₂ (10%, 100 molar equivalents) was added to the
42
43 cuvette. The solution was mixed and the absorption at 576 nm was recorded for the time of 500
44
45 s. Data points were recorded every 0.5 s.

46
47 *Bulk degradation of 1 by H₂O₂.* To 75 mL of a borax buffer solution of **1** (30 mg, 0.16 mmol) at
48
49 pH 10 H₂O₂ was added (30%, 195 molar equivalents). Upon complete decolouration, a 10 %
50
51 solution of Na₂S₂O₃ was added dropwise until the excess peroxide was destroyed. A 15 mL
52
53 aliquot of the solution was used for the GC-MS analysis. The remaining 60 mL were frozen at -
54
55 80°C and lyophilized and used for NMR experiments in D₂O. For *in situ* NMR experiments, the
56
57 reaction set up was repeated in a smaller scale with 30 equivalents of H₂O₂ (30%). The solution
58
59
60

1
2
3 was not lyophilized, but directly analyzed under application of a water suppression technique. ^1H
4 NMR ($\text{H}_2\text{O}+\text{D}_2\text{O}$): δ 8.45 (s, **7**), 6.12 (bs, unknown), 6.10 (s, **3**), 3.60 (s, **4**), 3.14 (s, **6**), 1.99 (s,
5 **8**). ^{13}C δ 184.6 (**8**, COOH), 174.6 (**4**, COOH), 176.9 (**3**, COOH), 173.7 (**7**, COOH), 132.8 (**3**,
6 CH=CH), 54.1 (**4**, $\text{CH}_2(\text{O})$), 49.7 (**6**, CH_2), 26.4 (**8**, CH_3)
7
8
9

10
11
12 *GC-MS analysis.* A 15 mL aliquot of the **1**/ H_2O_2 bulk degradation solution was used for the GC-
13 MS analysis of degradation products. The sample pH was adjusted to neutral by addition of HCl.
14 200 μL of the sample solution were added to a GC vial for freeze-drying. Standard addition,
15 derivatization and sample analysis were performed according to the literature procedure reported,
16 as were the GC-MS operating conditions.¹⁹ The NIST/Wiley 2008 database was used for
17 compound identification.
18
19
20
21
22

23
24
25 *EPR measurements.* The intermediates were generated by rapid mixing of DHNQ (28 mM) with
26 H_2O_2 (5%, 5 molar equivalents) in a solution of buffer pH 10/MeCN (1:1) and immediately
27 transferred to a quartz flat cell in the EPR cavity. Then the acquisition of EPR spectra was started
28 with the following parameters: microwave frequency, 9.76 GHz; microwave power, 20 mW;
29 receiver gain, 4.48×10^5 ; modulation frequency, 100 kHz; modulation amplitude, 2 G; center field,
30 3479.4 G; sweep 20 G; scan rate, 28.6 G/min; time constant, 327 ms; data points, 1024;
31 temperature, 300 K; 15 scans were recorded. Simulation of EPR spectra was performed with the
32 program WINSIM.²³ Simulation parameters: Lorentzian 0.640, G-shift -0.186, line width 0.848.
33 Coupling constant. (2+2) equivalent protons: 2.277 Hz.
34
35
36
37
38
39
40
41

42
43 *Degradation of 1 under conditions applied in EPR - in situ NMR.* **1** (5.3 mg, 0.028 mM) was
44 dissolved in 0.6 mL of a 1:1 mixture of borax buffer (pH 10) and MeCN. A few drops of D_2O
45 and 4,4-dimethyl-4-silapentane-1-sulfonic acid (DSS) as an internal standard were added. H_2O_2
46 (5%, 5 molar equivalents) was added and the solution immediately used for ^1H NMR
47 experiments under application of a water suppression technique. The solution was kept at r.t. for
48 6 days and measured again in NMR and EPR. ^1H NMR ($\text{H}_2\text{O}:\text{MeCN}=1:1+\text{D}_2\text{O}$): δ 8.40 (s, **7**),
49 7.27 (bs, radical), 6.52 (bs, radical), 6.45 (s, **1**), 6.06 (s, **3**), 3.52 (s, **4**), 3.31 (s, **6**)
50
51
52
53
54
55
56
57
58
59
60

1
2
3
4
5
6
7
8
9
10
11
12
13
14
15
16
17
18
19
20
21
22
23
24
25
26
27
28
29
30
31
32
33
34
35
36
37
38
39
40
41
42
43
44
45
46
47
48
49
50
51
52
53
54
55
56
57
58
59
60

*Synthesis of 1,4,5,8-naphthalenetetrone (I₂).*¹⁵ **1** (76 mg, 0.40 mmol) was dissolved 5 ml of a 1:1 mixture of acetone and acetonitrile. [Bis(trifluoroacetoxy)iodo]benzene (516 mg, 1.2 mmol) was added stepwise and upon complete addition, the solution stirred at r.t. for 3 hours. The solution was concentrated and addition of acetone yielded **I₂** (19 mg, 25%) by precipitation. UV/Vis (MeCN): λ_{\max} [nm] (log ϵ) 556 (0.36), 514 (0.67), 485 (0.72), 286 (2.42). ¹H NMR (CD₃CN): δ 6.85 (s, 4 H). ¹³C NMR: δ 186.6 (C-1/ C-3/ C-6/ C-8), 137.0 (C-2/ C-7), 127.6 (C-4/C-5/ C-9/ C-10).

Degradation of I₂ by H₂O₂. 5.7 mg (30 μ mol) of **I₂** were dissolved in 0.8 ml of borax buffer (pH 10). H₂O₂ (30%, 10 equivalents) was added. After 3 hours, 100 μ l of D₂O and DSS as an internal standard were added to the reaction mixture. The solution was transferred into a NMR tube and the spectra recorded using a water suppression technique. ¹H NMR (H₂O/D₂O): δ 8.44 (s, 1H, **7**), 6.85 (s, 4 H, **2**), 6.24 (s, 2 H, **3**), 3.60 (s, 2H, **4**), 3.35 (s, 2H, **6**), 2.06 (s, 2H, **8**)

Computational methods. GAUSSIAN 09 was used in all calculations. The geometry optimization of **1** and energy calculation of the intermediate **R₁** were carried out by the DFT method with the M062x functional, PCM (“SCRF” key word) in water was applied. Geometry optimisations and frequency calculations were performed by using the key word “Opt” and “Freq”. The 6-31G(d) basis sets were used for H, C, and O, applied by the key words “6-311+G(d)” for C and “6-311G(d,p)” for H.

Acknowledgement

The authors would like to thank the Austrian Research promotion Society (FFG, project 829443) for financial support and Dr. Nora Odabas for many fruitful discussions.

Supporting Information. The supporting information file contains computational data of compounds **1**, **1_a**, **R₁**, **R₀** and **H₂O₂**, NMR spectra of the degradation experiments as well as MS spectra of the degradation product.

References

1. Korntner, P.; Hosoya, T.; Dietz, T.; Eibinger, K.; Reiter, H.; Spitzbart, M.; Roeder, T.; Borgards, A.; Kreiner, W.; Mahler, A. K.; Winter, H.; Groiss, Y.; French, A. D.; Henniges, U.; Potthast, A.; Rosenau, T. *Cellulose* **2015**, *22*, 1053.
2. Rosenau, T.; Potthast, A.; Krainz, K.; Yoneda, Y.; Dietz, T. Shields, Z. P. I.; French, A. D. *Cellulose* **2011**, *18(6)*, 1623.
3. Rosenau, T.; Potthast, A.; Milacher, W.; Hofinger, A.; Kosma, P. *Polymer* **2004**, *45*, 6437.
4. Hosoya, T.; Rosenau, T. *J. Org. Chem.* **2013**, *78*, 3176.
5. Hosoya, T.; Rosenau, T. *J. Org. Chem.* **2013**, *78*, 11194.
6. Hosoya, T.; French, A. D.; Rosenau, T. *Mini-Rev. Org. Chem.* **2013**, *10*, 309.
7. Sandman, D. J. *Mol. Cryst. Liq. Cryst.* **2006**, *461*, 147.
8. Atkins, P.; de Paula, J. *Atkins' Physical Chemistry, 7th Edition*; Oxford University Press, 2002. $\Delta H = E_a - (R \times T)$, $\Delta G = R \times T \times [23.760 + \ln(T/k)]$, $\Delta S = [(E_a - R \times T) - \Delta G]/T$
9. Mikova, H.; Rosenberg, M.; Kristofikova, L. *Chem. Listy* **2001**, *95*, 28.
10. Ina, T.; Nippon Shokubai Co., Ltd., Japan, JP2014070028A, 2014, p. 8.
11. Yoshino, S.; Hayakawa, K.; Kanematsu, K. *J. Org. Chem.* **1981**, *46*, 3841.
12. Rosenau, T.; Potthast, A.; Zwirchmayr, N. S.; Hettegger, H.; Plasser, F.; Hosoya, T.; Bacher, M.; Krainz, K.; Dietz, T. *Cellulose* **2017**, *24*, 3671-3687.
13. Rosenau, T.; Potthast, A.; Kosma, P.; Hosoya, T.; Henniges, U.; Mereiter, K.; French, A. D. *Cellulose* **2017**, *24*, 1227.
14. Rosenau, T.; Potthast, A.; Kosma, P.; Saariaho, A.-M.; Vuorinen, T.; Sixta, H. *Cellulose* **2005**, *12(1)*, 43.
15. Maxted, D. R. *J. Chem. Soc.* **1926**, 2178.
16. Gille, L.; Nohl, H. *Arch. Biochem. Biophys.* **2000**, *375*, 347.
17. Lubitz, W.; Feher, G. *Appl. Magn. Reson.* **1999**, *17*, 1.
18. Duling, D. R. *J. Magnet. Reson. Ser. B* **1994**, *104*, 105.
19. Liftinger, E.; Zweckmair, T.; Schild, G.; Eilenberger, G.; Boehmdorfer, S.; Rosenau, T.; Potthast, A. *Holzforschung* **2015**, *69*, 695.